



Use of Waste Rubber and Bionanofiller in Preparation of Rubber Nanocomposites for Friendly Environmental Flooring Applications



B. K. Saleh, S. A. El Mogy*

Polymer Metrology and Technology Department, National Institute of Standards (NIS), Giza, Egypt.

ONE major environmental problem that cannot be solved on a large scale is the tire waste. Such tires accumulate to form waste mountains which cannot be easily handled. This study suggests a solution, if succeeded, that consumes half of this waste, when applied. The waste tire powder (WTP) is blended with natural rubber (NR) then mixed with a natural bionanofiller in the ratio of 1:1. This bionanofiller is the rice husk nanoparticles (RH-NPs) it was made by ball milling technique then added to WTP/NR in different concentrations; 0, 1.25, 2.5, 5.0, and 10.0 phr to give WTP/NR nanocomposites. Another batch was prepared in which the RH-NPs were mixed with an unsaturated polyester resin adhesive (PEA). The effect of adding PEA in addition to RH-NPs on the prepared nanocomposites was also investigated. Morphological studies via SEM analysis revealed that, at low content of RH-NPs (2.5wt.%), the RH-NPs were homogeneously dispersed in the nanocomposite matrices. TGA analysis declared that the addition of RH-NPs enhanced the thermal stability of WTP/NR nanocomposites, especially for those containing PEA. Mechanical tensile properties including tensile strength, Elongation modulus and elongation at break percent lead us to the same results. Results of testing the antimicrobial activity showed that the addition of the bionanofiller had a significant effect in enhancing the antimicrobial activity (AMA) against *Staphylococcus aureus* (*S. aureus*) bacteria, while the use of PEA affected badly AMA. Thus, the addition of RH-NPs in low percentages to WTP/NR composites enhances the mechanical, abrasion, thermal insulation properties as well as compression set. The prepared nanocomposites show antibacterial activity against *S. aureus*. This study offers a solution to manage a serious environmental problem by with a potential of being safely used in flooring applications such as kinder garden, hospitals and school playgrounds.

Keywords: Waste tire powder/natural rubber blend, Rice husk bionanofiller, Unsaturated polyester adhesive, Scanning electron microscopy, Mechanical, thermal and antimicrobial properties.

Introduction

Recycling of waste rubber has constantly created serious attention worldwide as the increases of these wastes have posed negative impacts on the environment. Rubber wastes are usually land-filled. There are efforts to reduce the depletion of natural resources and save the landfill space [1,2]. Irzaman and coworkers prepared biosilica from rice husk by HCl acid treatment [3], Numerous researches had been directed to find new

approaches for rubber wastes recycling. Some of these approaches might involve the incorporation of recycled rubber crumbs as composites into concrete material [4,5], asphalt mixture [6,7,8] and insight on pyrolytic carbon black [8]. Crumb rubber is effective in dissipating impact energy when it is used in composite preparation [4]. The other alternative direction is oriented to the need for large areas to accommodate this huge remaining part of waste [10]. The accumulation of waste tires in landfills increases the risk of

*Corresponding author e-mail: soma.elmogy@yahoo.com

Received 2/12/2019; Accepted 16/12/2019

DOI: 10.21608/ejchem.2019.20433.2225

©2020 National Information and Documentation Center (NIDOC)

their combustion, which pollutes the environment and natural resources due to its highly toxic emissions [11]. Previous studies demonstrated that waste tire rubber can be utilized in concrete as partial replacement of its mineral aggregate, preserving natural resources and decreases the number of waste tires entering landfills [11,12]. According to Sodupe-Ortega et al. [13], the waste tire can be used as a lightweight aggregate for the manufacture of concrete components to enhance the thermal and sound properties. Fattuhi and Clark [14] recommended that cement-based materials containing WTP can be used in many applications such as jersey barriers, lightweight concrete blocks, sea defense, armor units, pile heads, paving slabs, floor screeds, trench filling, pipe bedding, and artificial reef construction. The author and co-workers partially replaced carbon black by organomodified nanoclay [14] and crumb rubber. They studied also the effect of adding various concentrations of crumb rubber on the mechanical and thermal properties of organo - modified nanoclay filled WTP/NR nanocomposites. They found that the properties were improved at a 1:1 ratio of WTP: NR [15,16]. NR and synthetic rubbers are converted to serviceable products by combining them with fillers [17]. The natural fillers (biofillers) have a great deal of attention from researchers due to new resource, lightweight, low cost, non-toxic, eco-friendly, comparable properties to synthetic fillers [18-22]. Rice husk is one of these biofillers. It is a waste that results from rice harvest process which leaves two major wastes one of them is rice husks. These wastes obtained as waste of the rice milling process [23]. A minor quantity of RH is usually consumed in feeding sheep and cattle, while the major quantity is burnt without taking any precautions to protect the air or people, and giving rise to what is known as the Black Cloud at the period from September to November of every year. Recently, significant efforts have been done to investigate the use of RH as a reinforcing biofiller [24-26]. Therefore, the use of RH in polymer-based composites may represent a beneficial solution. Like most of fillers, RH is hydrophilic in nature and its chemical analysis showed that RH includes cellulose (35%), hemicellulose (25%), lignin (20%), ash (17%), and others (3%) by weight [24,27,28]. The hydrophilic nature of fillers makes them very sensitive towards water absorption which decreases the mechanical properties of the composite to a great extent [24]. This problem can be handled by the use of

adhesives or coupling agents. The polar groups of the adhesive are able to interact with functional groups on the filler, while its long hydrocarbon tails are able to anchor to the polymer matrix through physical entanglements and van der Waals interactions [26]. A bridge between the filler and the matrix is thereby established. Visconte et al [29] investigated the effect of the coupling agent, bis (3-triethoxysilylpropyl)-tetrasulfide (Si-69), on the curing and physical properties of the natural rubber. They found that the presence of the silane coupling agent showed an increase in the properties. Mounir et al [30] rice husk flour filler/polypropylene (RH/PP) composites with different ratios of the filler were prepared without and with maleated PP. The results indicated that the interfacial bonding between RH and PP was enhanced by the presence of the coupling agent, and the thermal stability of the grafted PP was enhanced by the grafting process. The main objective of this study is to prepare eco-friendly nanocomposites that can be used for flooring applications. This will be carried out by replacing conventional fillers by RH in its nano-sized form and by adding this filler with different concentrations (1.25, 2.5, 5 and 10 phr) to 1:1 by weight of WTP/NR blends.

Materials and Methods

Materials

Rice husk was obtained from a local rice mill, Egypt. Crumb rubber (waste tire powder, WTP) was obtained from the 6th. October Co., Egypt. Natural rubber (NR) was brought from Transportation and Engineering Co., Alex., Egypt. Unsaturated polyethylene resin (PEA) was from the local market. It has an acid value of 23, specific gravity (at 20 °C) of 1.12, and styrene content of 40%. It is used as a coupling agent to improve the mechanical properties of the nanocomposites. The rubber chemicals consisted of zinc oxide (ZnO), stearic acid, processing oil, N-Cyclohexyl-2-benzothiazole Sulfenamide (CBS), Tetramethylthiuram Disulfide (TMTD), N-(1,3-dimethylbutyl)-N'-phenyl-p-phenylenediamine (6PPD), and sulfur. All materials were of commercial grade and were used as received.

Preparation of RH-NPs

A laboratory ball milling machine was used to reduce the particle size of RH particulates to powder in the nanoscale range (RH-NRs). The powder was sieved using a laboratory sieve and the average particle size was < 100 nm.

Fourier Transform Infrared (FTIR) Spectroscopy

A thin film of RU-NPs by mixing (0.002g) with KBr were compression molded to give to form a round disk suitable for FT-IR analysis. FTIR spectroscopy was carried out using a Nicolet 380 spectrophotometer (Thermo Scientific) and the IR spectra were scanned over the wave number range of 4,000–400 cm⁻¹.

Preparation of RH-NPs/WTP/NR nanocomposites

A master batch was prepared according to the mix formulations as tabulated in Table 1. NR was firstly masticated using a laboratory two-roll mill (152.4 × 330.2 mm) at a friction ratio of 1:1.4. The nip gap, roll speed ratio, and a number of passes were kept the same for all of the mixes. The distance between the two rolls varied during the addition of additives. WTP was added to masticated NR in the ratio of 1:1. Zinc oxide and stearic acid were added to the WTP/NR blend before adding the curing system. 6PPD was used as an antioxidant. PEA was added to the RH-NPs/WTP/NR mixes to study its effect in enhancing the interfacial bonding between RH and WTP/NR and hence to improve the properties of the resulting nanocomposites. RH-NPs were added in different amounts; 1.25, 2.5, 5 and 10 phr in order to study the role of RH-NPs as a filler in the WTP/NR composites. Mixing was carried out in accordance with ASTM D3182-16. The compounding ingredients of all composites are given in Table (1).

Cure characteristics

The rheometer properties were determined with an oscillating disk rheometer (Alpha Technologies MDR 2000) working at 150°C.

The cure characteristics of the different mixes; maximum torque (M_H), minimum torque (M_L), scorch time (t_{s2}) and the optimum cure time (T_{c90}) were recorded. The difference in torque ($\Delta M = M_H - M_L$) and the cure rate index were calculated. The cure rate index (CRI) of all WTP/NR nanocomposites was calculated according to the following formula [31]:

$$CRI = 100 / (t_{90} - t_{52}) \quad (1)$$

The prepared samples for testing were compression molded in a laboratory hydraulic press (Mackey Bowley, C1136199) at 150°C at a pressure of 13.5 MPa according to ASTM D2084-17. Dumbbell shape samples of thickness 2.5 mm were cut from the compressed sheets using standard cutter according to ASTM D 412-16.

Thermal analysis (TGA)

Thermal Gravimetric Analysis (TGA) of all WTP/NR nanocomposites was carried out using Shimadzu-50 Thermogravimetric Analyzer in presence of air, using temperature range of 25 °C to 650 °C with a rate of 10°C. The degradation temperature of the composites was studied through this analysis.

Scanning Electron Microscopy (SEM)

In this study, the analysis was performed to study the fracture surface of WTP/NR nanocomposite. The effect of modification with PEA on the RH-NPs/WTP/NR nanocomposite was studied using SEM (JEOL-JSM-5500, Japan). Before testing, all samples were coated with a thin layer of gold using a gold sputter coater (SPI – module).

TABLE 1. Compounding ingredients of WTP/NR nanocomposites composites.

Ingredients, phr	B ₀	BU1	BU2	BU3	BU4	BM1	BM2	BM3	BM4
NR	50	50	50	50	50	50	50	50	50
WTP	50	50	50	50	50	50	50	50	50
RH-NPs	0	1.25	2.5	5	10	1.25	2.5	5	10
PEA	0	0	0	0	0	5	5	5	5
Zinc Oxide	5	5	5	5	5	5	5	5	5
Stearic Acid	2	2	2	2	2	2	2	2	2
Processing Oil	5	5	5	5	5	5	5	5	5
6PPD	1	1	1	1	1	1	1	1	1
CBS	1	1	1	1	1	1	1	1	1
TMTD	1.5	1.5	1.5	1.5	1.5	1.5	1.5	1.5	1.5
Sulfur	2	2	2	2	2	2	2	2	2

Mechanical properties

For measuring the mechanical properties of the rubber vulcanizates, sheets of dimensions 200 mm × 200 mm × 2 mm were prepared using a hydraulic press under a pressure of 13.5 MPa. Dumbbell shaped samples were cut from the molded sheets. Modulus, tensile strength, and elongation at break were determined using a Zwick (model Z010, Germany) tensile testing machine at a temperature of 23 ± 2°C and a crosshead speed of 500 mm/min according to ASTM D412-16.

Abrasion Resistance Measurements

The abrasion test has measured the resistance of a material to wear resulting from rubbing, grinding, or scraping against another material. IT is expressed as an abrasion loss in cubic Millimetre or abrasion resistance index in percent. The abrasion resistance of the composites was performed according to ASTM D53516 using Zwick abrasion tester (Material Prufung). It was calculated according to the following equation:

$$A = \frac{(\Delta m \cdot S_o)}{(\rho \cdot S)} \quad (2)$$

where A is the abrasion loss in mm³, Δm is the loss in mass (mg), ρ is the density of rubber (g/cm³), S_o is the nominal abrasive grade (200 mg), and S is the abrasive grade in mg.

Compression set measurements

Cylindrical samples of dimensions 22 mm diameter and 10 mm thickness were molded in the hydraulic press at 150°C. A compression set device consists of four steel plates between which the samples are compressed. The plates are held together by three axial bolts. Ring-shaped spacers of different thicknesses, 6.00, 7.614 and 9.228 mm, are placed around three axial bolts [32]. The different thicknesses (I_s) of the spacers help to control the degree of compression. After placing the samples, in between the steel plates, the bolts were tightened firmly over the samples. The compression set was accommodated in an air circulating oven at 70°C for 48 hours. After then, it is removed from the oven and allowed to cool. Then, the samples were released and allowed to recover for half an hour before measuring the final thickness accurately. The compression and

recovery percentage was calculated using the following relations:

$$\text{Percentage compression set, C \%} = \frac{I_o - I_r}{I_o - I_s} \times 100 \quad (3)$$

where I_o is the sample initial thickness, I_r is the sample thickness after recovery and I_s is the spacer thickness.

Determination of Antibacterial activity

The microorganisms used in the study consisted of the reference strains from the American Type Culture Collection (ATCC) belonging to 6 Gram-positive bacteria (Staphylococcus aureus bacteria (*S. aureus*) ATCC 25923. *S. aureus* was used to determine the antibacterial activity of the modified/unmodified natural rubber nanocomposites. The bacterial cultures were maintained on Nutrient Agar (NA) slants. The test bacterial suspensions (100 mL) were spread on NA plates. Freshly prepared samples were cut into squares with the diameter being 5.5 mm, which would be put in the seeded plates. The samples were initially incubated for 15 min (to allow diffusion) and later on at room temperature for 48 h for the bacterial cultures. Positive test results were scored when a halo of inhibition was observed around the WTP/NR nanocomposites samples after the incubation.

Results and Discussion

FT-IR Analysis

FTIR spectra of raw RH was shown in Figure 1. Table (2) presented infrared adsorption wavelength range and the corresponding functional groups that were recognized in the FTIR spectra of raw rice husk. The FTIR analysis revealed a peak at 3726 cm⁻¹ which resulting from the free and intermolecular hydroxyl groups stretching vibration. Two peaks were seen at 3398 cm⁻¹ and 2910 cm⁻¹ showed the (-NH) and (-CH) stretching vibration, respectively. The presence of a peak at 2360 cm⁻¹ showed NH₂ bending vibration. The presence of a peak around 1625 cm⁻¹ and 1365 cm⁻¹ confirmed (-CO) and (-COO) stretch vibration. Presence of intense band at 1072 cm⁻¹ can be assigned to the C-O of alcohols and carboxylic acids. Peak around 891 cm⁻¹ shows the presence of (-CH₂) bending. This result is in agreement with other authors [33].

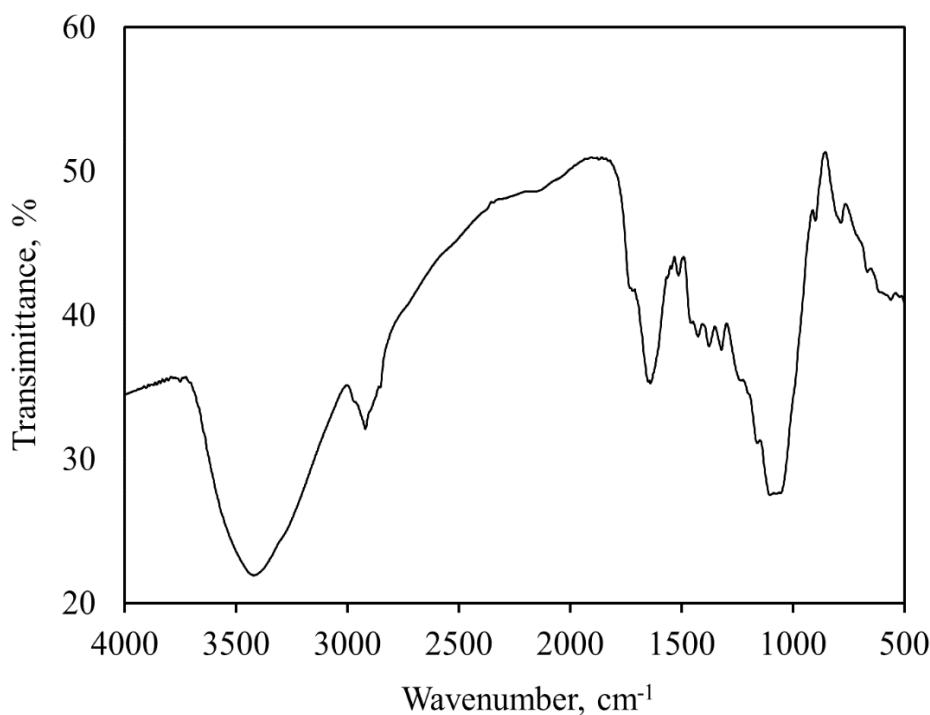


Fig.1. FTIR of raw RH-NPs.

TABLE 2. Range of IR wavelength (cm^{-1}) with respect to the functional group from FTIR spectra of raw rice husk.

IR Range	Functional group	Functional moiety	Data from the curve
3750-3000	Free and intermolecular-OH	OH stretch	3726
3520-3320	NH_2 in aromatic amines	NH stretch	3398
2990-2850	CH_3 and CH_2 in aliphatic compound	CH stretch	2910
2700-2250	Amine salts	NH_2 stretch	2360
1680-1620	O and NH_2 in primary amides	C O stretch	1625
1400-1310	COO^- group in carboxylic acid	Antisym. stretch	1365
1060-1025	$\text{CH}_2\text{-OH}$ in primary alcohols	C O stretch	1072
950-865	CH-CH_2 in vinyl compounds	CH_2	891

Rheological characteristics

Table (3) summarized the cure parameters of WTP/NR nanocomposites containing different concentrations of RH-NPs both unmodified and modified with unsaturated polyester resin. Scorch time (t_{s_2}) is the time in min. when the premature vulcanization of the material occurs. From the values of the scorch time in Table (3), it can be seen that there is an increase in scorch time with the increase of RH-NPs content in WTP/NR nanocomposite and reaching maximal values for mixes having 2.5 g of RH-NPs for both unmodified and modified WTP/NR mixes. This may be attributed to the viscosity

decrease with the increase of RH-NPs content in WTP/NR mixes due to the formation of some crosslinks at the beginning of the vulcanization process. Therefore, a longer time was required for the beginning of the vulcanization process. It is worthy to mention that the scorch time for modified nanocomposites is longer than that of the unmodified showing the effect of adding the applied adhesive for enhancing the premature vulcanization stage. The minimum torque (M_L) is a measure of the stiffness of the unvulcanized rubber composite as indicated by the lowest point of the cure curve. The values of M_L in Table (3) declared that the minimum torque increased with increasing the RH-NPs concentration. This increase reaches a maximum value at 2.5 g of

RH-NPs for unmodified nanocomposites while it continues to increase with RH-NPs loading for the modified nanocomposites reflecting the effect of the adhesive in increasing the stiffness of the nanocomposite mix. This is in accordance with the increase in scorch time and the viscosity increase due to crosslinking formation before curing. The maximum torque (M_H) is a measure of stiffness or shear modulus of the fully vulcanized test specimen at vulcanization temperature. In other words, it is also an indicator of the crosslink density of rubber; the higher the M_H value, the higher the crosslink density [34]. (ΔM) or delta torque is defined as the difference between the maximum and minimum torque. From Table (3), it is clear that both M_H and ΔM increased with the increase of RH-NPs addition. This is can be explained on the basis that the successively increased formation of crosslinks between the macromolecular chains, as a result of adding more RH-NPs, leads to an increase in the viscosity of the fully vulcanized WTP/NRs, especially for those having higher contents of RH-NPs. The cure time (t_{90}), defined as the time needed for the mix to reach 90 % of the whole vulcanization process, decreases with the increase of the RH-NPs loading up to 2.5 g. This decrease is because the RH-NPs plays a role in accelerating the vulcanization process up to 2.5 g. Further increase in RH-NPs loading to WTP/NR mixes leads to an increase in the cure time. Although the addition of RH-NPs accelerates the vulcanization process, its addition in excess takes more time for the formation of more crosslinks leading again to an increase in cure time at higher levels of RH-NPs. A similar conclusion can be obtained from the values of the cure rate index (CRI) given in Table (3).

Thermal Gravimetric Analysis TGA

High-temperature Thermal Analysis (TGA) is always performed to explore the thermal stability of

rubber composites against temperature elevation. Being a thermoset, rubber composites decompose or degrade to give fumes and lose weight. The higher the values of the temperature are the more stable the composite will be. The temperature for the onset of degradation (T_{10}) is the temperature at which the composite under testing loses 10% of its original during the analysis. The temperature at which 50% degradation occurs is denoted as (T_{50}) and the temperature at which 90 % degradation occurs is given the symbol (T_{90}). The weight loss percent (WL %) is the ratio of the remaining solid mater to the original weight at the end of the test. These data were calculated from the TGA plots. Table (4) describes the behavior of vulcanized WTP/NR nanocomposites towards temperature upraise at temperature range 50-650 °C. It was observed that all WTP/NR nanocomposite samples reveal high onset degradation temperature levels showing that the addition of RH-NPs enhances the thermal stability, especially for those modified with the polyester resin as represented in the the values of the weight loss in Figure (2). The onset degradation temperature T_{10} showed a steady increase in its values with leveling up the RH-NPs concentration. This continues to reach a maximum value of up to 2.5 loadings. This increase can be attributed to the increase in the crosslink density. The crosslinking increases the rigidity of the rubber mix, which in turn increases the thermal stability [35]. The addition of more RH-NPs causes a decrease in T_{10} reflecting the decrease in the thermal stability of the nanocomposite as a result of RH-NPs agglomeration and imperfect dispersion in the nanocomposite matrix. For T_{50} and T_{90} temperature values, they both show similar behavior. This is in good agreement with the results obtained from SEM analyses and the values of maximum torque. Thus the addition of RH-NPs to WTP/NR mixes improves their stability towards thermal decomposition and the

TABLE 3. Rheological characteristics of WTP/NR nanocomposites containing unmodified and modified RH-NPs.

Sample Property	Unmodified					Modified			
	Bo	BU1	BU2	BU3	BU4	BM1	BM2	BM3	BM4
M_L , Kg.cm	0.03	0.04	0.05	0.02	0.01	0.04	0.05	0.05	0.07
M_H , Kg.cm	9.22	6.32	9.32	11.75	12.13	8.18	9.89	9.84	11.17
ΔM , Kgm.cm	9.19	6.27	9.28	11.73	12.12	8.14	9.84	9.79	11.10
T_{S2} , min	1.12	1.16	1.18	1.16	1.10	1.15	1.23	1.20	1.11
T_{c90} , min	2.37	2.21	2.19	2.37	2.31	2.02	2.00	2.36	2.20
CRI, min ⁻¹	80.00	95.20	99.00	82.60	82.60	93.50	129.90	94.30	91.70

TABLE 4. Effect of adding different loadings of RH-NPs on the thermal stability of WTP/NR nanocomposites.

Mix Property	Unmodified					Modified			
	Bo	BU1	BU2	BU3	BU4	BM1	BM2	BM3	BM4
T ₁₀ , °C	312.1	315.1	318.3	316.0	314.3	326.7	349.8	341.2	339.6
T ₅₀ , °C	314.2	320.0	329.8	321.2	318.3	333.9	371.3	352.7	347.2
T ₉₀ , °C	381.0	391.4	409.3	402.8	395.2	415.6	456.4	429.3	422.1
WL %	43.9	43.4	41.9	42.3	43.0	40.2	34.4	38.6	39.9

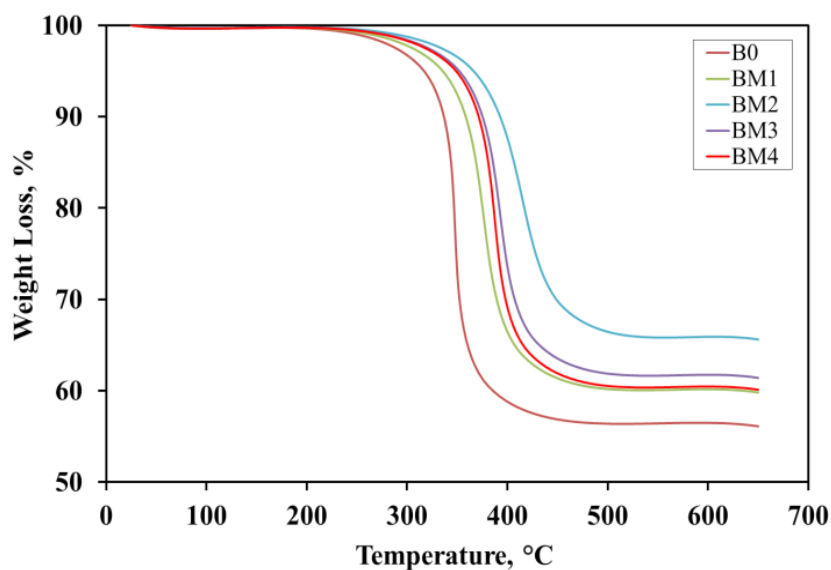
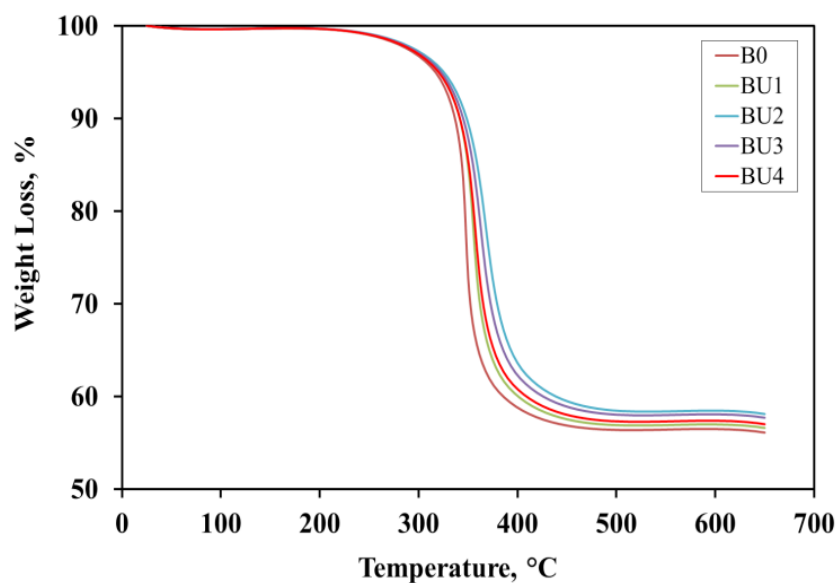


Fig.2. TGA thermographs for WRP/NR nanocomposites: a) Unmodified; b) Modified.

addition of the polyester adhesive gives rise to higher stability levels.

Scanning electron microscopy of the fractured surface

SEM is an important tool for studying the fractural morphology for rubber compounds. In our study the morphological characterization was carried out to evaluate how far the WRP/NR blends and all other ingredients, including RH-NPs, from compatibility and good dispersion in the nanocomposite matrix. The fractural morphologies of the WTP/NR nanocomposites Bo, BU2, BM2, BU4 and BM4 were examined by SEM and shown in Figure (3a-e). Compared to the control composite represented by Figure (3a), nano composites containing RH-NPs showed poor dispersion of RH in the nanocomposite with the increase in the loading of RH-NPs Figure (3b,d). This explains the lowering the mechanical properties and Abrasion resistance for these nanocomposites with the increase RH-NPs content in the WTP/NR nanocomposites. Figure (3c,e) represent the SEM for that same nanocomposites but in presence of the UPE adhesive. The size of the aggregates was greatly reduced and a better uniformity was achieved. The RH-NPs were homogeneously dispersed in the nanocomposites with no large defects observed in the fractured view of the blends. Thus, PEA played an effective role in improving the dispersion of RH in the nanocomposites. The results give a true reflex of how the bio-nanofiller particles interact with the WTP/NR nanocomposites that affect the overall properties of the blends.

Mechanical properties

The mechanical properties of all unmodified and modified WTP/NR vulcanizes are tabulated in described in Figure (4a-c). These properties include the results of the maximum tensile strength (TS), the elastic modulus (E-Modulus) and elongation at break percentage (E-Break %). It is clear that the tensile strength increases with the increase of the RH-NPs addition reaching a maximum value at 2.5 phr of RH-NPs for both unmodified and modified WTP/NR nanocomposites. This increase indicates the good impact of adding RH-NPs in enhancing the dispersion of all ingredients, as well as good interaction in the WTP/NR, which is higher for modified RH-NPs than the unmodified ones. Further addition of RH-NPs results in a drastic drop in the TS values of both unmodified and modified nanocomposites. This drop is because RH-NPs resemble the NR-Ps in its effect when present in excess in reducing the TS of

nanocomposites. This was attributed to the presence of agglomerated nanoparticles that has the tendency for splitting [36,37]. Similar trends were noticed with regarding E-Modulus and E-Break %. The increase in E-modulus values continues to till the RH-NPs loading reach 2.5 phr. This is due to the increase in the crosslink density of the vulcanizates at levels below 2.5 g of RH-NPs. This is evidential from the results of the maximum torque from rheological measurements.

Abrasion Loss measurements

Since the aim of this article is to prepare a nanocomposite that can be used in flooring applications, it is essential to study the Abrasion trend of all the prepared nanocomposites. The abrasion resistance of the material is defined as the ability to withstand abrasion by means of friction such as rubbing, scratching or erosive action [38]. This test was performed to measure the effect of adding different loadings of the RH-NPs bio-nanofiller to WTP/NR the abrasion loss. Figure (5) showed the effect of adding different concentrations of RH-NPs on the weight loss of WTP/NR nanocomposites. Results showed the abrasion loss of all WTP/NR nanocomposites with and without the adhesive resin. Generally, it can be seen that the addition of RH-NPs to WTP/NR raises the abrasion loss levels of all nanocomposites. This continues to happen and reaches its maximal values for nanocomposites having 2.5 g bio-nanofiller. These results are in good agreement with the torque values that had been discussed above in the rheological part. The higher the torque values are, the higher the abrasion resistance will be [39]. Also, Rattanasom et al. [40] reported that the abrasion resistance was related to the hardness and the crosslink density. This trend stops and nanocomposites exhibit a decrease in abrasion loss with further bio-nanofiller upload to WTP/NR nanocomposites.

Compression Set Properties

When a product is compressed and then allowed to relax, it will recover to its original dimension; this variation from its original form is called the compression set. The compression set is a measure of rubber ability to retain its elastic property after a prolonged compression at a constant strain under the specified condition, and it is a permanent set of rubber compounds [41,42]. To determine the effect of adding different RH-NPs loading to WTP/NR on the compression set

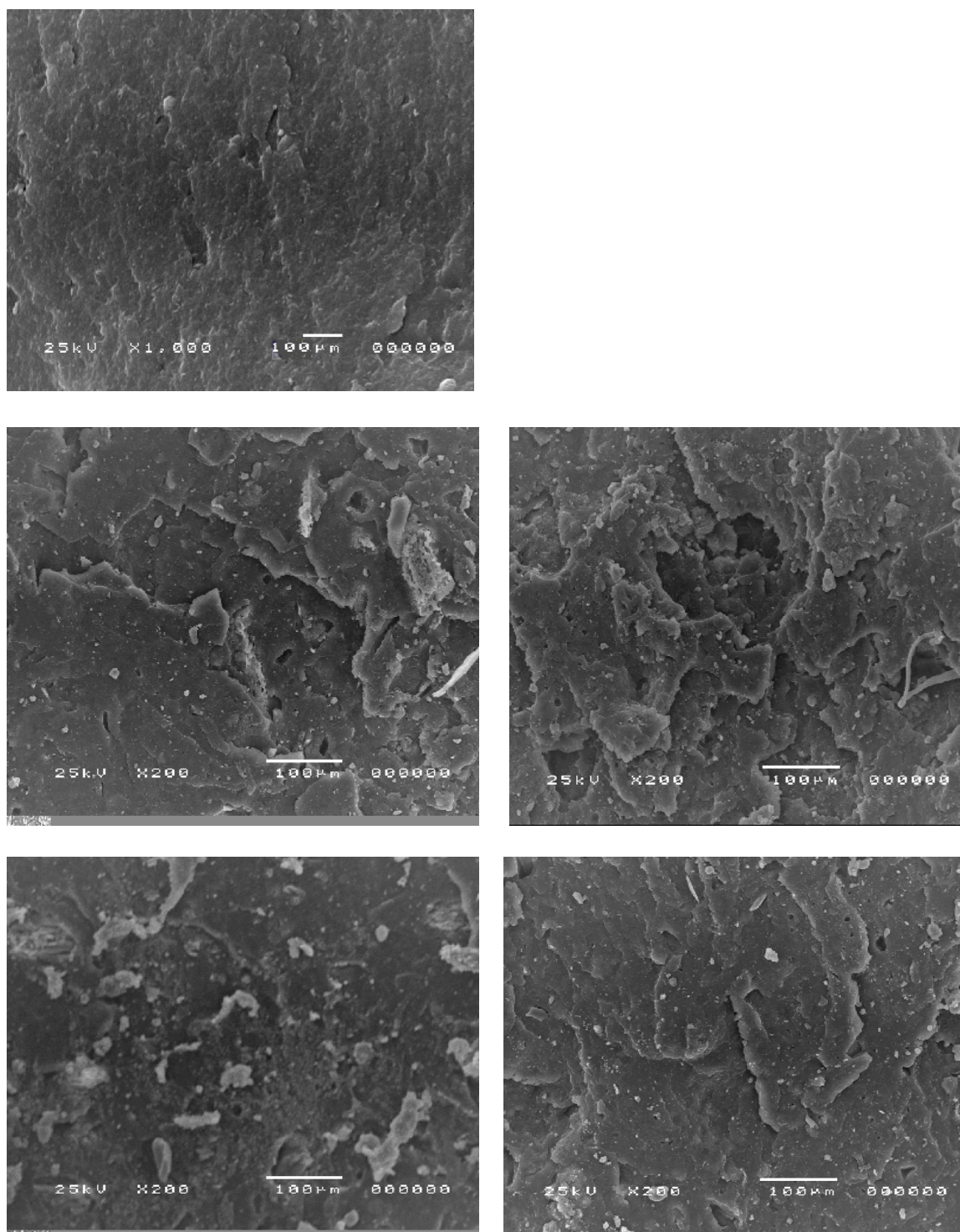


Fig. 3. SEM micrographs of WTP/NR nanocomposites with different content of RH-NPs: a) Bo, b) BU2, c) BM2, d) BU4, e) BM4.

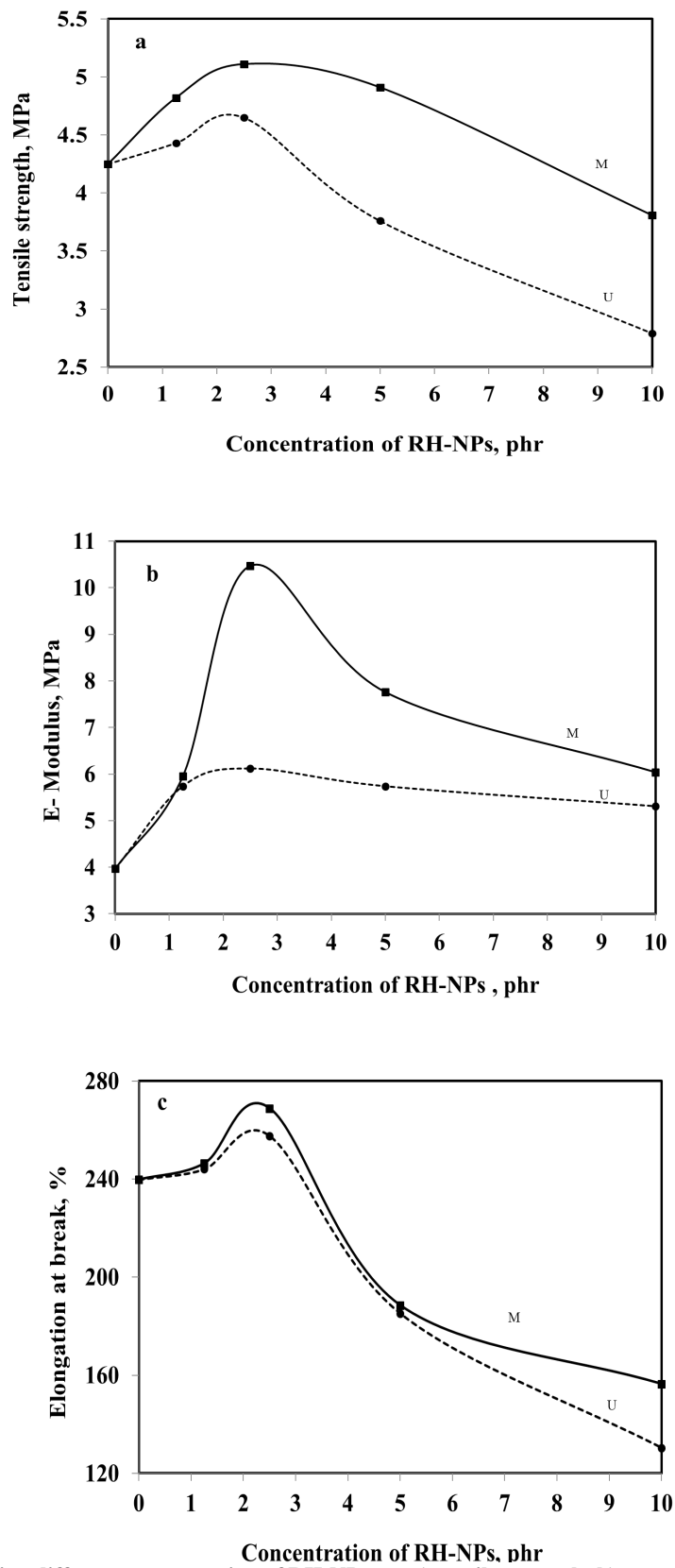


Fig. 4. Effect of adding different concentration of RH-NPs on: a) tensile strength; b) e- modulus and c) elongation at break..

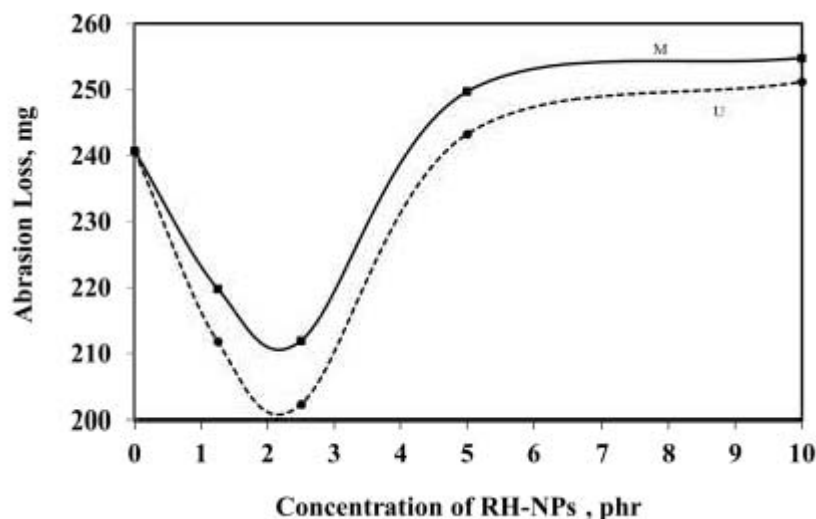


Fig. 5. Effect of adding different concentration of RH-NPs on the weight loss of WTP/NR nanocomposites.

behavior of NR/CR compounds, the compression set test was carried out at 70°C for 48 hours.

The experimental results are shown in Figure (6). This Figure showed the variation of the percentage of compression set against RH-NPs loading (wt.%) to WTP/NR nanocomposites compounds in the absence and presence of PEA adhesive. From this Figure, it is clear that in the case of the reference composite (Bo), the compression set is low. Upon increasing the RH-NPs, the compression set increases and reaches a maximum value for WTP/NR nanocomposites with 2.5 wt % of RH-NPs. This is because as the RH-NPs loading concentration increase in the polymer, the void space reduced in the composite and hence mobility of polymer matrix of decreased. Therefore, induce stiffness in the RH-NPs filled compounds resulting in a high percentage of compression set [43,44]. The increase in compression set value means that the memory retainable capacity of composites decreases. However, a decreasing trend in the compression set can be seen when the RH-NPs loading was further increased to 10 wt.%. In the presence of PEA, the value of the compression set increased. This is due to the addition of the PEA improved the interfacial bonding between the fiber and the compound. The lower values of compression set reflect better retained elastic properties [45]. So it can be concluded that WTP/NR nanocomposite loaded with 10

wt.% RH exhibited the best compression set value.

Antimicrobial analysis

The ability of the green nanoparticles (RH-NPs) to inhibit the growth activity of the bacteria on the WTP/NR nanocomposite was evaluated. The results of the antimicrobial activity were tested against *S. aureus* ATCC 25923 and were described in Figure (7) and the inhibition activity of RH-NPs based WTP/NR was expressed as a function of the inhibition zone. Table (5) summarizes the antibacterial inhibition activity by tabulating the size of the inhibition zone. From Table (5) and Figure (7), it is clear that WTP/NR blend possesses antibacterial inhibition activity and it is represented by an inhibition zone of 23 mm, Figure (5a). This activity may be due to WTP blended with NR. The antimicrobial activity was improved with the addition of RH-NPs in different amounts. The addition of the bionanofiller had a significant effect in enhancing the antimicrobial inhibition activity (AMA) against *S. aureus* bacteria. When RH-NPs was added (2.5 wt. %) to WTP/NR blend, the bacterial growth was inhibited expressed by the clear inhibition zone whose size is 25 mm. The inhibition zone increases to 32 mm with the increase in the RH-NRs amount to 10 phr reflecting an obvious improvement in the antibacterial inhibition activity. This can be explained on the basis that 60 % of RH is mainly cellulose and hemicellulose which possess many OH groups. The polar nature of RH is responsible for the antibacterial growth inhibition. Unfortunately, the addition of the adhesive decreases the number of OH groups and affected badly the inhibition activity

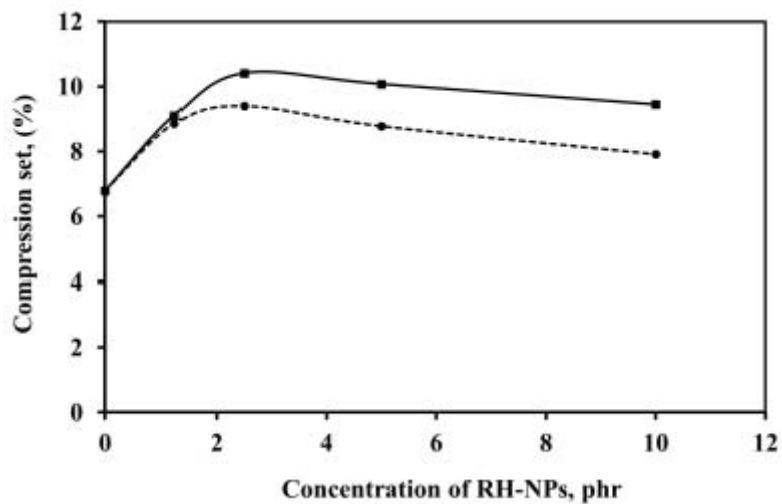


Fig. 6. Effect of adding different concentration of RH-NPs on the compression set of WTP/NR nanocomposites .

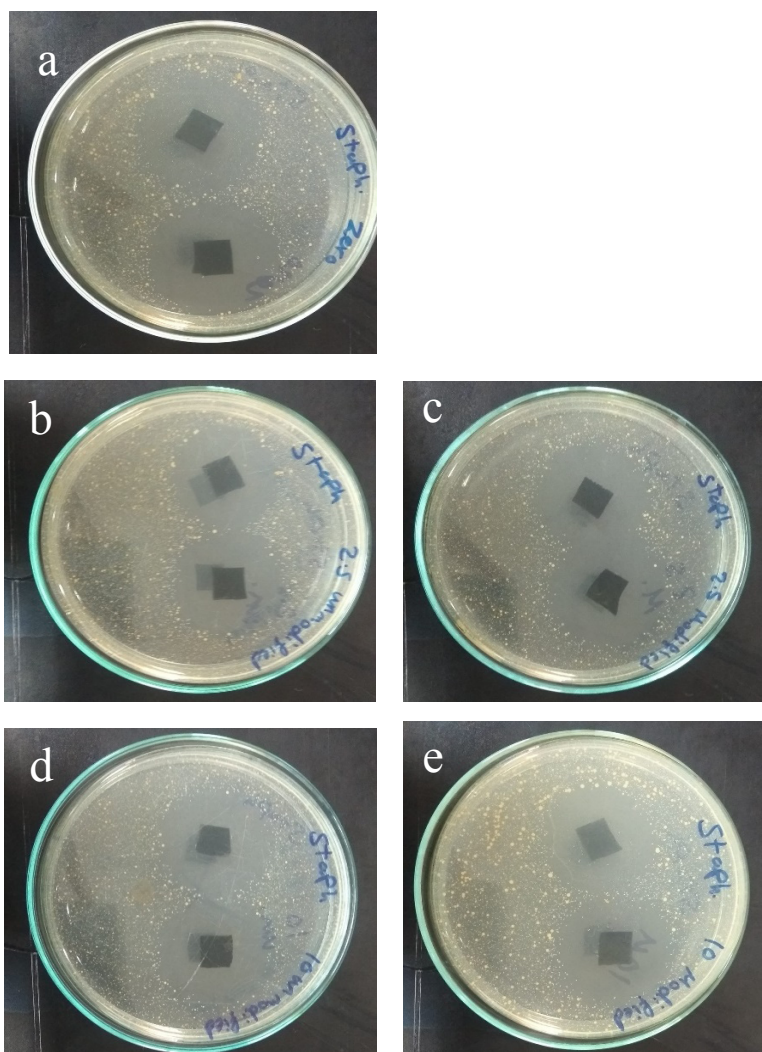


Fig. 7. Images of the antimicrobial activities against *Staphylococcus aureus* bacteria of WTP/NR nanocomposites with different amounts of RH-NPs.

TABLE 5. Inhibition zone of RH filled NR/AC blends against antibacterial agent after 48 h. of incubation .

Sample	The diameter of inhibition zone (mm)
Bo	23
BU2	25
BU4	32
BM2	20
BM4	20

to a limit lower than that was observed by WTP/NR without RH-NPs [46].

Conclusion

It is important to clarify in this study that green and cost-effective reinforcement and antibacterial nanomaterial was developed. It can be used for flooring, medical applications, and hospital instruments hoses as antibacterial rubber. Natural rubber/water tire powder nanocomposites based on rice husk nanoparticles were prepared via two roll mill and their properties were evaluated. The content of RH-NPs was varied and the results were compared with the neat sample without the addition of filler. Scorch time was improved with the increase in RH-NPs content, while cure time decreased with increasing RH-NPs content. The addition of RH-NPs improved the thermal stability of WTP/NR nanocomposites and the addition of the PEA adhesive a better stability level. Mechanical properties were enhanced at low concentrations of RH-NPs. Antibacterial resistance was enhanced by the addition of RH-NPs against *S. aureus* while, the addition of PEA causes a dramatic decrease in antibacterial activity.

References

- Rashad A.M., A comprehensive overview about recycling rubber as fine aggregate replacement in traditional cementitious materials, *International Journal of Sustainable Built Environment*, 5, 46-82, (2016).
- Depaolini A.R., Bianchi G., Fornai D., Cardelli A., Badalassi M., Cardelli C. and Davoli E., "Physical and chemical characterization of representative samples of recycled rubber from end-of-life tires", *Chemosphere*, 184, 1320-1326, (2017).
- Irzaman Irzaman; Indah Dwi Cahyani; Aminullah Aminullah; Akhiruddin Maddu; Brian Yulianto; Ulfah Siregar, *Egyptian Journal of Chemistry*, Volume 62, special issue (part 1), December, pp. 27-28 (2019).
- Medina N. F., Medina D. F., Olivares F. H., and Navacerrada M. A., "Mechanical and thermal properties of concrete incorporating rubber and fibres from tire recycling", *Construction, and Building Materials*, 144, 563-573, (2017).
- Youssef O., Hassanli R. and Mills J.E., "Mechanical performance of FRP-confined and unconfined crumb rubber concrete containing high rubber content", *Journal of Building Engineering*, 11, 115-126, (2017).
- Gonzalez P. L., Perez M.A.C., Fresno D.C., Zamanillo A.V. and Vega I. I., "Porous asphalt mixture with alternative aggregates and crumb-rubber modified binder at reduced temperature", *Construction and Building Materials*, 150, 260-267, (2017).
- Huang W., Lin P., Tang N., Hu J. and Xiao F., "Effect of crumb rubber degradation on components distribution and rheological properties of Terminal Blend rubberized asphalt binder", *Construction and Building Materials*, 151, 897-906, (2017).
- Zhu X., Miao C., Liu J., and Hong J., "Influence of crumb rubber on frost resistance of concrete and effect mechanism" *Procedia Engineering*, 27, 206 – 213, (2012).
- Berki P., Gobl R. and Kocsis J.K., "Structure and properties of styrene-butadiene rubber (SBR) with pyrolytic and industrial carbon black", *Polymer Testing*, 61, 404-415, (2017).
- Suparat, T., "Waste Tyre Management in Thailand: a Material Flow Analysis Approach", *Asian Institute of Technology*, School of Environment. Resources and Development, Thailand, (2013).
- Guelmine, L., Hadjab, H., Benazzouk, A., "Effect of elevated temperatures on physical and mechanical properties of recycled rubber mortar" *Construct. Build. Mater.* 126, 77-85, (2016).
- Guoqiang Li, Gregory Garrick, John Eggers, Christopher Abadie, Michael A. Stubblefield, Su-Seng Pang, Waste tire fiber modified concrete., *Egypt. J. Chem.* 63, No. 7 (2020)

- Compos. B Eng.* 35, 305-312, (2004).
13. Sodupe-Ortega E., Fraile-Garcia E., Ferreiro-Cabello, J., Sanz-Garcia A., "Evaluation of crumb rubber as aggregate for automated manufacturing of rubberized long hollow blocks and bricks" *Construct. Build. Mater.* 106, 305-316, (2016).
 14. Fattuhi, N.I., Clark, L.A., "Cement-based materials containing shredded scrap truck tire rubber", *Construct. Build. Mater.* 10, 229-236, (1996).
 15. Saleh. B. K., Hanna S. F., Khalil M.H., "Evaluation of thermal and mechanical properties of crumb/natural rubber nanocomposites" *Egyptian Journal of Chemistry*, In Press.
 16. Saleh. B. K., Khalil M.H., "Study on the role of crumb rubber on the thermal and mechanical properties of natural rubber nanocomposites", *Egyptian Journal of Chemistry*, 60, 1205 – 1214, (2019).
 17. Asore E.J. "An Introduction to Rubber Technology, First Edition, Josen Books, Benin City, (2000).
 18. George J., Sreekala M.S., and Thomas S., "A review on interface modification and characterization of natural fiber reinforced plastic composites", *Polymer Engineering & Science*, 41, 1471-1485, (2001).
 19. Saheb D.N. and Jog J.P., "Natural fiber polymer composites: A review", *Advances in Polymer Technology*, 18 351-363, (1999).
 20. Satyanarayana K.G., Arizaga G.G.C., and Wypych F., "Biodegradable composites based on lignocellulosic fibers-An overview", *Progress in Polymer Science*, 34, 982-1021, (2009).
 21. Yang H. S., Wolcott M., Kim H. S., Kim S., and Kim H. J., "Properties of lignocellulosic material filled polypropylene bio-composites made with different manufacturing processes", *Polymer Testing*, 25, 668-676, (2006).
 22. Yang H. S., Wolcott M., Kim H. S., Kim S., and Kim H. J., "Effect of different compatibilizing agents on the mechanical properties of lignocellulosic material filled polyethylene bio-composites", *Composite Structures*, 79, 369-375, (2007).
 23. Park B. D., Wi S. G., Lee K. H., Singh A. P., Yoon T. H., and Kim Y. S., "Characterization of anatomical features and silica distribution in rice husk using microscopic and micro-analytical techniques", *Biomass and Bioenergy*, 25, 319-327, (2003).
 24. Nouri M. R., Dogouri F. J., Oromiehie A., and Langroudi A. E., "Mechanical properties and water absorption behaviour of chopped rice husk filled polypropylene composites", *Iranian Polymer Journal*, 15, 757-766, (2006).
 25. Demir H., Atikler U., Balköse D., and Tihminlioglu F., "The effect of fiber surface treatments on the tensile and water sorption properties of polypropylene-luffa fiber composites", *Composites Part A: Applied Science and Manufacturing*, 37, 447-456, (2006).
 26. Yang H. S., Kim H. J., Park H. J., Lee B. J., and Hwang T. S., "Effect of compatibilizing agents on rice-husk flour reinforced polypropylene composites", *Composite Structures*, 77, 45-55, (2007).
 27. Premalal H. G. B., Ismail H., and Baharin A., "Comparison of the mechanical properties of rice husk powder filled polypropylene composites with talc filled polypropylene composites", *Polymer Testing*, 21, 833-839, (2002).
 28. Panthapulakkal S., Sain M. and Law S., "Effect of coupling agents on rice husk filled HDPE extruded profiles", *Polymer International*, 54, 137-142, (2005).
 29. Da Costa H. M., Visconte L. L. Y, Nunes R. C. R, Furtado C. R. G., "The Effect of Coupling Agent and Chemical Treatment on Rice Husk Ash- Filled Natural Rubber Composites", *Journal of Applied Polymer Science*, Vol. 76, 1019–1027, (2000).
 30. Mounir El Sayed M., Shehata A. B., Darwish N. A., Abd El Megeed A. A, Badawy N. A., El-Bayaa A. A., El-Mogy S. A."Effect of Compatibilizing Agents on the Mechanical Property of Rice Husk Flour as Nano-Potential Filler in Polypropylene Biocomposite", *Journal of Applied Polymer Science*, 125, 1310–1317, (2012).
 31. Aral M. M. and Taylor S. W., "Ground water quantity and quality management", *ASCE publications*, United State of America, 494, (2011).
 32. Lawandy, S. N., Halim S. F., Afifi H. A., "Ultrasonic and Mechanical Measurements for the Detection of Crosslink Density of SBR and NBR Based on Various Curing Systems", *J. Appl. Polym. Sci.*, 112, 366–371, (2009).
 33. Sarma, P. J., Kumar, R., and Pakshirajan, K., "Batch and Continuous Removal of Copper and

- Lead from Aqueous Solution using Cheaply Available Agricultural Waste Materials”, *Int. J. Environ. Res.*, 9(2):635-648, Spring (2015).
34. Hassan A. and Haworth B., *J. Material Processing and Technology*, 172, 341-345, (2006).
35. Maity M., Khatua B.B., Das C.K., “Effect of processing on the thermal stability of the blends based on polyurethane: part IV”, *Polym. Degrad. Stab.*, 72: 499, (2000).
36. Liu Y. and Kontopoulou M., “The structure and physical properties of polypropylene and thermoplastic olefin nanocomposites containing nanosilica”, *Polymer*, 47, 7731-7739, (2006).
37. LI J. X., SILVERSTEIN M., HILTNER A, and BAER E., “The ductile-to-quasi-brittle transition of particulate-filled thermoplastic polyester:., *J. Appl. Polym. Sci.*, 52 No. 2, 255-267, (1994).
38. Zhu G. Ji, H., Qi C., and Zeng Z., “*Polym. Eng. Sci.*”, 49, 1383, (2009).
39. Arayaprane W. and Rempel G. L.,” *J. Appl. Polym. Sci.*, 110, 1165, (2008).
40. Rattanasom N., Saowapark T. and Deeprasertkul C., “*Polym. Test*”, 26, 369, (2007).
41. Smith L. P.,”The language of rubber”. Butterworth, Heinemann, London, (1993).
42. Othman A. B., “Property profile of a laminated rubber bearing”, *Polym. Test* 20:159-166, (2001).
43. Vishvanathperumal S., Gopalakannan S.,”Effects of the Nanoclay and Crosslinking Systems on the Mechanical Properties of Ethylene-propylene-diene Monomer/styrene Butadiene Rubber Blends Nanocomposite”, *Silicon*, 11:117-135, (2019).
44. Schuur M. V.D., Gaymans R. J. “Influence of chemical crosslinks on the elastic behavior of segmented block copolymers”, *Polymer*, 46: 6862-6868, (2005).
45. Okiemen F.E., Imanah J. E., “physico-mechanical and equilibrium swelling properties of natural rubber filled with rubber Seed Shell Carbon”, *J. Polym Mater.* 22(4):409, (2005).
46. Abdulkhani A., Hosseinzadeh J., Ashori A., Esmaeeli H., “Evaluation of the antibacterial activity of cellulose nanofibers /polyacetic acid composites coated with ethanolic extract of propolis”, *Polymer Composites*, pp. 13-19, (2017).

إستخدام نفايات المطاط والمواد المألثة الحيوية في تحضير متراكبات المطاط النانوية لتطبيقات الأرضيات الصديقة للبيئة

بسمه كمال صالح، سومه أحمد السيد

المعهد القومي للقياس والمعايرة- الجيزه - مصر.

إن فضلات إطارات السيارات تمثل خطراً كبيراً على البيئة، حيث تتراكم هذه الإطارات في صورة جبال من الإطارات التالفة. إن هذه الدراسة تقترح حل قد يستهلك كميات كبيرة من هدم الفضلات. يتم عمل مزيج من مسحوق هذه المواد والمطاط الطبيعي بنسبة 1:1، وإضافة جزيئات قش الأرز النانوية لها مواد مالئة بنسب مختلفة ودراسة الخواص المختلفة لهذه المتراكبات النانوية. هذا بالإضافة إلى استخدام راتنج البولي إستر الغير مشبع كمادة لاصقة ودراسة خواصها الأخرى. وقد أوضحت النتائج أن إضافة جزيئات قش الأرز النانوية أسهمت في توزيع المكونات المضافة إلى المتراكبات بصورة جيدة أدت إلى زيادة تجانس المتراكبات النانوية بصورة كبيرة. وينعكس هذا التجانس بصورة إيجابية على الخواص الميكانيكية والعزل الحراري ومقاومة البري هذا بالإضافة إلى تحسن مقاومة هذه المتراكبات للبكتيريا. إن هذه الدراسة تقدم حل جيد لإدارة مشكلة بيئية خطيرة تساهم في التخلص من بقايا الإطارات من خلال الإستخدام الآمن لها في صناعة الأرضيات الخاصة برياض الأطفال، المستشفيات وملاعب كرة القدم.